

# Oxide ion conductivity in $(\text{Ba}_{0.3}\text{Sr}_{0.2}\text{La}_{0.5})(\text{In}_{1-x}\text{M}_x)\text{O}_{2.75}$ ( $\text{M} = \text{Sc}$ and $\text{Yb}$ ) systems

Katsuyoshi KAKINUMA,<sup>†‡</sup> Tetsuaki WAKI, Hiroshi YAMAMURA and Tooru ATAKE\*

Department of Material and Life Chemistry, Faculty of Engineering, Kanagawa University,  
3-27-1, Rokkakubashi, Kanagawa-ku, Yokohama 221-8686

\*Materials and Structures Laboratory, Tokyo Institute of Technology, 4259, Nagatsuta-cho, Midori-ku, Yokohama 226-8503

We have investigated the crystal phase and oxide ion conductivity of  $(\text{Ba}_{0.3}\text{Sr}_{0.2}\text{La}_{0.5})(\text{In}_{1-x}\text{M}_x)\text{O}_{2.75}$  ( $\text{M} = \text{Sc}$  and  $\text{Yb}$ ) systems as a function of dopant content and unit cell free volume. All peaks in the XRD diffraction patterns of these systems ( $x = 0.0 - 0.4$ ) were found to be assignable to pure cubic symmetry. The lattice parameter of the Sc-doped system decreased monotonically with rising dopant content, while the Yb-doped one showed a monotonic increase. The oxide ion conductivity of these systems increased with a unit cell free volume. Above a volume of  $2.43 \times 10^{-2} \text{ nm}^3$ , the oxide ion conductivity decreased. The oxygen vacancy content of the systems was controlled to be constant over the whole compositional range, which suggests that the mobile oxygen content should also be constant over the whole range. Above a free volume of  $2.43 \times 10^{-2} \text{ nm}^3$ , a broad Raman mode emerged from  $350 \text{ cm}^{-1}$  to  $400 \text{ cm}^{-1}$ , which might relate to the local distortion of oxygen octahedra. We conclude that the oxide ion mobility grows with increasing unit cell free volume up to a critical volume, and then the mobility is degraded by the local distortion of the oxygen octahedra.

©2009 The Ceramic Society of Japan. All rights reserved.

Key-words : Oxide ion conductivity, Perovskite oxide, Unit cell free volume

[Received January 22, 2009; Accepted March 17, 2009]

## 1. Introduction

Fast oxide ion conductors are important materials for use as electrolytes in solid oxide fuel cells, oxygen sensors, and oxygen-permeable membrane reactors.<sup>1)-4)</sup> In particular, the perovskite system comprises a group of attractive oxide ion conducting materials. The chemical formula of such an oxide is  $\text{ABO}_3$ : the A-site cation is 12-coordinate, and the B-site is 6-coordinate. An appropriate aliovalent substitution for the A and B-site cations can result in the generation of oxygen vacancies in the system, which would enhance its oxide ion conductivity.  $\text{LaGaO}_3$ -based perovskite oxides show a high oxide ion conductivity when co-doped with divalent Sr and Mg ions at the La and Ga sites, respectively.<sup>5),6)</sup> Another oxide ion conductor is the  $\text{Ba}_2\text{In}_2\text{O}_5$ -based oxides, discovered by Goodenough in 1990.<sup>7)</sup> The system is one of the Brownmillerite oxides, which are derived from perovskites. One-sixth of the oxygen in the unit cell is removed; because the oxygen vacancies are in an ordered state, the compound exhibits low oxide ion conductivity under 1203 K. Above that temperature, an order-disorder transition of the oxygen coordination occurs in the system, and, due to the disordering of the oxygen vacancies, high oxide ion conductivity appears. The oxide ion conductivity in the high temperature range exceeds that of yttria-stabilized zirconia (YSZ). Many studies have been conducted to attempt to make the oxide ion arrangement disordered under 1203 K, with the aim of improving the oxide ion conductivity, but none has reported a conductivity exceeding that of YSZ.<sup>8)-10)</sup> In our previous studies, fast oxide ion conductor of the

$(\text{Ba}_{0.3}\text{Sr}_{0.2}\text{La}_{0.5})\text{InO}_{2.75}$  system obtained by doping  $\text{La}^{3+}$  and  $\text{Sr}^{2+}$  into  $\text{Ba}_2\text{In}_2\text{O}_5$  was discovered. The conductivity of this system surpassed that of YSZ, and almost equaled that of the  $\text{LaGaO}_3$  system.<sup>11)-15)</sup> As concerns the oxide ion conducting mechanism of the  $\text{Ba}_2\text{In}_2\text{O}_5$  based oxide, Uchimoto et al. reported that the saddle point was the dominant conductivity factors in the  $\text{Ba}_2\text{In}_2\text{O}_5$  system.<sup>9)</sup> Ta et al. proposed that the oxide ion conductivity of the  $\text{Ba}_2\text{In}_2\text{O}_5$  based oxides depended on the dopant ion radius in case that the oxygen vacancy arrangement was in disordered state.<sup>16)</sup>

We reported that the oxide ion conductivity in any cation doped  $\text{Ba}_2\text{In}_2\text{O}_5$  system increased with unit cell free volume, and that the conductivity decreased with increasing free volume above a given free volume. Hayashi et al. and Nomura et al. also reported that the oxide ion conductivity in the other perovskite oxides behaved similarly versus unit cell free volume, and that the dependency would rely on the balance between the tolerance factor and the free volume.<sup>17),18)</sup>

In order to elucidate the reason for the unit cell free volume dependency on the oxide ion conductivity in any cation-doped  $\text{Ba}_2\text{In}_2\text{O}_5$  system, we paid attention to the crystallographic symmetry of the system. We selected  $\text{Sc}^{3+}$  and  $\text{Y}^{3+}$  cations as dopants for the In site to maintain the oxygen vacancy content of the system and to change the lattice parameter monotonically. We investigated the relationships between the oxide ion conductivity of the trivalent cation-doped  $(\text{Ba}_{0.3}\text{Sr}_{0.2}\text{La}_{0.5})\text{InO}_{2.75}$  system, the crystal symmetry and the local distortion.

## 2. Experimental

The samples were prepared by solid state reaction. The starting materials,  $\text{BaCO}_3$  (99.9%, Wako Pure Chemical Industries, Ltd.),  $\text{SrCO}_3$  (99.9%, Wako Pure Chemical Industries, Ltd.),  $\text{La}_2\text{O}_3$  (99.99%, Wako Pure Chemical Industries, Ltd.),  $\text{In}_2\text{O}_3$  (99.95%, Kojundo Chemical Laboratory Co., Ltd.),  $\text{Yb}_2\text{O}_3$  (99.9%, Kojundo

<sup>†</sup> Corresponding author: K. Kakinuma; E-mail: kkakinuma@yamanashi.ac.jp

<sup>‡</sup> Present address: Fuel Cell Nanomaterials Center, University of Yamanashi, 4-3-11, Takeda, Kofu, Yamanashi 400-8510

Chemical Laboratory Co., Ltd.), and  $\text{Sc}_2\text{O}_3$  (99.9%, Kojundo Chemical Laboratory Co., Ltd.) were mixed in a ball mill for 24 h with ethanol as a medium. The mixture was dried at 373 K for several hours, and then calcined at 1273 K for 10 h. The powder, which was sieved to under 54  $\mu\text{m}$ , was uniaxially pressed at 5 MPa into a rectangular shape (30 mm  $\times$  5 mm  $\times$  5 mm) and then isostatically pressed again at 200 MPa. The samples were then sintered at 1673 K for 10 h in air. The relative densities of all of the sintered specimens, estimated from their dimensions and weight, were higher than 90%. The single phase nature of the samples was confirmed by X-ray diffractometry with Cu  $\text{K}\alpha$  radiation (monochromated with graphite Multiflex, Rigaku Co.) at room temperature.

Four platinum wires were wound around the samples. Platinum paste was coated on each platinum wire and then sintered at 1223 K for 1 h in air. The electrical conductivity of the sintered samples was measured by the DC four-probe method under various conditions over a range of temperatures between 873 K to 1273 K and with oxygen partial pressures ranging from  $1.0 \times 10^5$  to  $1.0 \times 10^{-15}$  Pa; these oxygen partial pressures were controlled by varying the composition of the gas mixture (Ar– $\text{O}_2$  or Ar– $\text{H}_2\text{O}$ ). Raman spectra were obtained with an NRS-1000 (JASCO Co.) spectrometer equipped with a Nd:YVO<sub>4</sub> laser (wavelength, 532 nm). The output power of the laser was 100 mW.

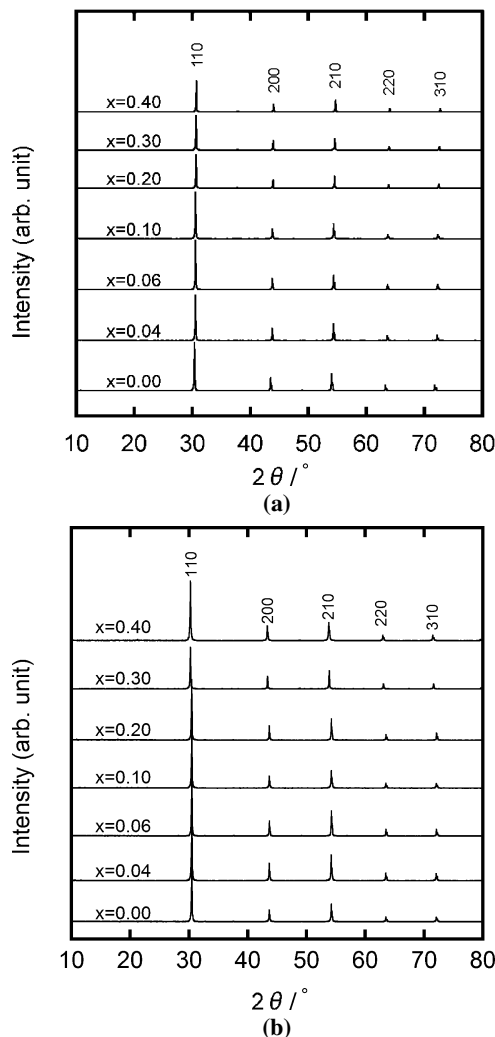


Fig. 1. XRD patterns of members of the  $(\text{Ba}_{0.3}\text{Sr}_{0.2}\text{La}_{0.5})(\text{In}_{1-x}\text{M}_x)\text{O}_{2.75}$  ( $\text{M} = \text{Sc}$  and  $\text{Yb}$ ) systems. (a)  $(\text{Ba}_{0.3}\text{Sr}_{0.2}\text{La}_{0.5})(\text{In}_{1-x}\text{Sc}_x)\text{O}_{2.75}$ , (b)  $(\text{Ba}_{0.3}\text{Sr}_{0.2}\text{La}_{0.5})(\text{In}_{1-x}\text{Yb}_x)\text{O}_{2.75}$ .

### 3. Results and discussion

The XRD patterns of the  $(\text{Ba}_{0.3}\text{Sr}_{0.2}\text{La}_{0.5})(\text{In}_{1-x}\text{M}_x)\text{O}_{2.75}$  ( $\text{M} = \text{Sc}$  and  $\text{Yb}$ ) systems are displayed in Figs. 1(a) and (b). Each peak in the XRD diffraction patterns was identified to be assignable to cubic symmetry. Uchimoto et al. found the La-doped  $\text{Ba}_2\text{In}_2\text{O}_5$  system to have cubic symmetry (space group,  $\text{Pm}3m$  No. 221).<sup>9)</sup> We labeled each XRD peak with reference to the symmetry and calculated the lattice parameter of the  $a$ -axis. The lattice parameters of these systems are shown in Fig. 2. The lattice parameter of the Sc-doped system decreased monotonically with increasing dopant content, whereas, the parameter of the Yb-doped system increased. The Shanon ionic radii of Sc, Yb and In are 0.0745 nm, 0.0868 nm and 0.0800 nm,<sup>19)</sup> respectively, which would affect the dopant content dependency of each lattice parameter.

In perovskite oxides, the electrons, oxide ions and holes function as charge carriers, so that the electrical conductivity of the oxide is the sum ( $\sigma_{tot}$ ) of the respective conductivities  $\sigma_e$ ,  $\sigma_o$  and  $\sigma_h$  as shown in Eq. 1.

$$\begin{aligned} \sigma_{tot} &= \sigma_e + \sigma_o + \sigma_h \\ &= \sigma_e^o P_{\text{O}_2}^{-n} + \sigma_o + \sigma_h^o P_{\text{O}_2}^{+m} \end{aligned} \quad (1)$$

Typical results of the electrical conductivity for the  $(\text{Ba}_{0.3}\text{Sr}_{0.2}\text{La}_{0.5})(\text{In}_{1-x}\text{M}_x)\text{O}_{2.75}$  ( $\text{M} = \text{Sc}$  and  $\text{Yb}$ ) system at 1073 K are shown as a function of oxygen partial pressure in Fig. 3. We found that electronic conductivity appeared for the  $x = 0$  system for  $\log[P_{\text{O}_2}(\text{Pa})] < -10$ . In the low oxygen partial pressure region,  $\text{In}^{3+}$  would be reduced to  $\text{In}^+$  and would supply the conducting electrons in the system. We also found that the electronic conductivity of the Sc- or Yb-doped system did not appear in the same oxygen partial pressure region. The electronic conductivity of the perovskite system follows the polaron hopping mechanism.<sup>20)–22)</sup> Polaron conduction appears due to the hopping of charge carriers between B sites in the perovskite system. A mixed valence conduction for the In cation would provide hopping sites for electrons in this system. However, the dopant cations of Sc and Yb are highly stable in the +3 state, so that they do not supply conducting electrons and do not permit the hopping sites for electrons. We conclude that the doped Sc or Yb cations would prevent the generation of conducting electrons and would interfere with the mobility of electron hopping at low oxygen partial pressures.

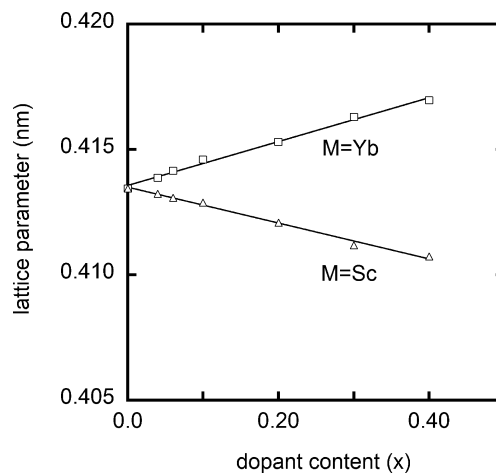


Fig. 2. Lattice parameters of members of the  $(\text{Ba}_{0.3}\text{Sr}_{0.2}\text{La}_{0.5})(\text{In}_{1-x}\text{M}_x)\text{O}_{2.75}$  ( $\text{M} = \text{Sc}$  and  $\text{Yb}$ ) systems.

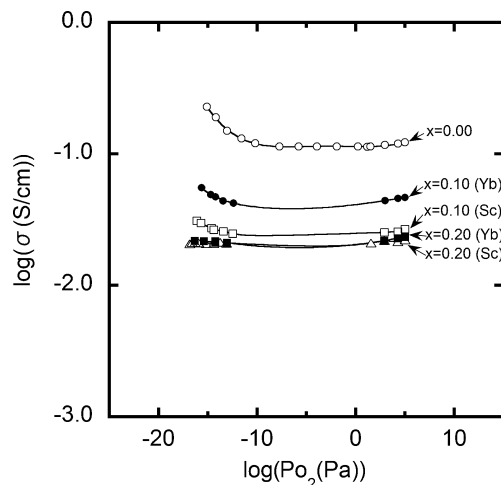


Fig. 3. Electrical conductivity of members of the  $(\text{Ba}_{0.3}\text{Sr}_{0.2}\text{La}_{0.5})(\text{In}_{1-x}\text{M}_x)\text{O}_{2.75}$  ( $\text{M} = \text{Sc}$  and  $\text{Yb}$ ) systems at 1073 K as a function of the oxygen partial pressure.

The electrical conductivities of all systems at 1073 K were independent of oxygen partial pressure in the region between  $\log[P_{\text{O}_2}(\text{Pa})] = 1.5$  and  $-11$ , suggesting that the transport number of oxide ion conductivity was unity at 1073 K in Ar atmosphere ( $\log[P_{\text{O}_2}(\text{Pa})] = 1.5$ ). The electrical conductivities from 873 K to 1173 K in Ar atmosphere are displayed as Arrhenius plots in Figs. 4(a) and (b). The activation energy of the oxide ion conductivity ranged from 82 to 97 kJ/mol, which is almost constant in the compositional region. We considered that the transport number of oxide ion conductivity in this system was unity from 873 K to 1173 K in Ar atmosphere, and that the oxide ion conductivity of all compositional region would show same dopant content dependency in the temperature region.

The oxide ion conductivities of the  $(\text{Ba}_{0.3}\text{Sr}_{0.2}\text{La}_{0.5})(\text{In}_{1-x}\text{M}_x)\text{O}_{2.75}$  ( $\text{M} = \text{Sc}$  and  $\text{Yb}$ ) systems as a function of dopant content at 1073 K are shown in Fig. 5. The oxide ion conductivities of both systems decreased with increasing dopant content and were similar in value for the same dopant content. The oxide ion conductivity is strongly dependent on the oxygen vacancy content and crystal characteristics, such as lattice parameter, crystal symmetry and dopant ion radius. These systems have the same oxygen content, but the lattice parameters of the Sc- and Yb-doped systems showed the opposite dopant content dependency, as displayed in Fig. 2. In order to understand the contradiction, we have paid attention to the other important crystallographic parameter – the unit cell free volume. This quantity is defined as the difference between the unit cell volume and the sum of the volumes of the component cations

$$\text{unit cell free volume} = a^3 - \sum_i m_i \frac{4}{3} \pi r_i^3 \quad (2)$$

where  $a$  is the cubic lattice parameter,  $m_i$  is the chemical composition ratio of a particular ion, and  $r_i$  is its ionic radius.<sup>19</sup> The oxide ion conductivity of the  $(\text{Ba}_{0.3}\text{Sr}_{0.2}\text{La}_{0.5})(\text{In}_{1-x}\text{M}_x)\text{O}_{2.75}$  ( $\text{M} = \text{Sc}$  and  $\text{Yb}$ ) system at 1073 K is shown as a function of the unit cell free volume in Fig. 6. We found that the oxide ion conductivity of the system increased with increasing unit cell free volume up to  $2.43 \times 10^{-2} \text{ nm}^3$ , and then decreased. As shown in Figs. 4(a) and (b), the Arrhenius plots of oxide ion conductivity was parallel to each other, so that the unit cell free volume dependency of oxide ion conductivity would show same behavior. The

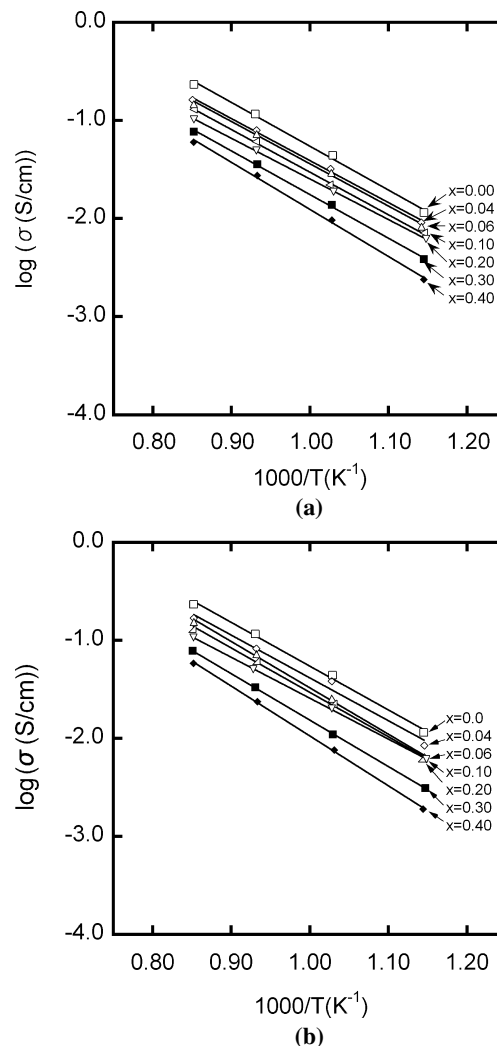


Fig. 4. Arrhenius plots of oxide ion conductivity for members of the  $(\text{Ba}_{0.3}\text{Sr}_{0.2}\text{La}_{0.5})(\text{In}_{1-x}\text{M}_x)\text{O}_{2.75}$ . ( $\text{M} = \text{Sc}$  and  $\text{Yb}$ ) systems. (a)  $(\text{Ba}_{0.3}\text{Sr}_{0.2}\text{La}_{0.5})(\text{In}_{1-x}\text{Sc}_x)\text{O}_{2.75}$ , (b)  $(\text{Ba}_{0.3}\text{Sr}_{0.2}\text{La}_{0.5})(\text{In}_{1-x}\text{Yb}_x)\text{O}_{2.75}$ .

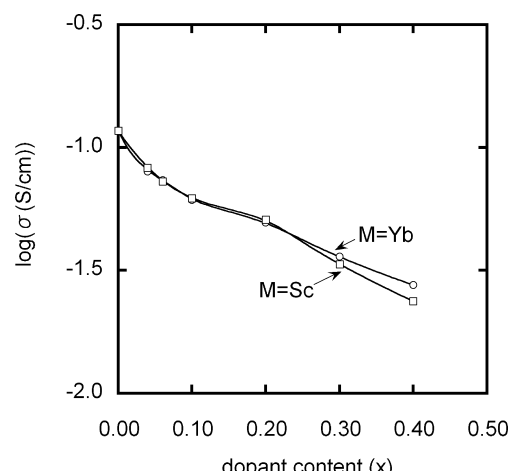


Fig. 5. Oxide ion conductivity at 1073 K as a function of dopant content.

oxygen vacancy content was constant in these systems, so we assume that the unit cell free volume dependency is related to the mobility of the oxide ion. The results shown in Fig. 6, therefore,

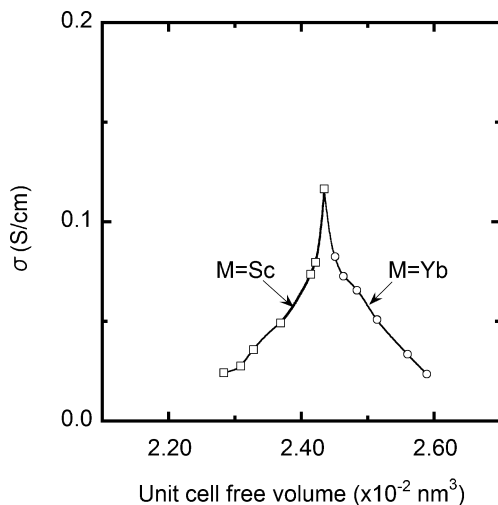


Fig. 6. Oxide ion conductivity at 1073 K as a function of unit cell free volume.

lead us to the conclusion that the oxide ion mobility of the system first increased with the unit cell free volume and then decreased due to the operation of other factors.

A possible reason for a decrease of the oxide ion conductivity is the ordering of component cations and anions, as seen in structures such as the pyrochlore-type oxide ion conductors<sup>23)</sup> and the parent  $\text{Ba}_2\text{In}_2\text{O}_5$  oxide ion conductor.<sup>7)</sup> In the case of perovskite oxides, a B-site cation ordering arrangement was reported in the perovskite-related oxide  $\text{Ba}_2\text{HoHfO}_{5.5}$ , which exhibited an XRD pattern that included superlattice reflections.<sup>24)</sup> However, such reflections are missing in the XRD data of the  $(\text{Ba}_{0.3}\text{Sr}_{0.2}\text{La}_{0.5})(\text{In}_{1-x}\text{M}_x)\text{O}_{2.75}$  ( $\text{M} = \text{Sc}$  and  $\text{Yb}$ ) system, shown in Figs. 1(a) and (b). Moreover, the X-ray diffraction peaks did not split with increasing cation doping, which suggested that the crystal symmetry did not change due to ordering of the oxide ions.

Another possible cause of the lowering of the oxide ion conductivity is a local distortion of the oxygen octahedra. Although the X-ray diffraction pattern is not sensitive to local distortions, Raman spectroscopy can detect local distortions and the presence of oxygen vacancies. The Raman spectra for the  $(\text{Ba}_{0.3}\text{Sr}_{0.2}\text{La}_{0.5})(\text{In}_{1-x}\text{M}_x)\text{O}_{2.75}$  ( $\text{M} = \text{Sc}$  and  $\text{Yb}$ ) system are displayed in Fig. 7. Even though there is no Raman-active mode in the case of cubic symmetry,<sup>25),26)</sup> we detected a mode around  $630 \text{ cm}^{-1}$ , which has been reported to be related to oxygen vacancies in perovskite oxides.<sup>27)-29)</sup> Moreover, the broad mode appeared from  $350 \text{ cm}^{-1}$  to  $400 \text{ cm}^{-1}$  above unit cell free volume values of  $2.43 \times 10^{-2} \text{ nm}^3$ . It was reported that the stretching mode of oxygen octahedral appeared around the same wave number in the perovskite oxide of  $\text{SrCeO}_3$  system, and that the broadening was corresponded to the local lattice distortion of the oxygen octahedra.<sup>30)</sup> Further work is needed to clarify the origin of the broad mode. We speculate that this Raman mode also might reflect local distortions for the oxygen octahedra of  $(\text{Ba}_{0.3}\text{Sr}_{0.2}\text{La}_{0.5})(\text{In}_{1-x}\text{Yb}_x)\text{O}_{2.75}$  system, and that such distortions might be the reason for the degradation of the oxide ion conductivity above unit cell free volumes of  $2.43 \times 10^{-2} \text{ nm}^3$ .

#### 4. Conclusion

We have synthesized single-phase samples of members of the  $(\text{Ba}_{0.3}\text{Sr}_{0.2}\text{La}_{0.5})(\text{In}_{1-x}\text{M}_x)\text{O}_{2.75}$  ( $\text{M} = \text{Sc}$  and  $\text{Yb}$ ) systems ( $x = 0.0$

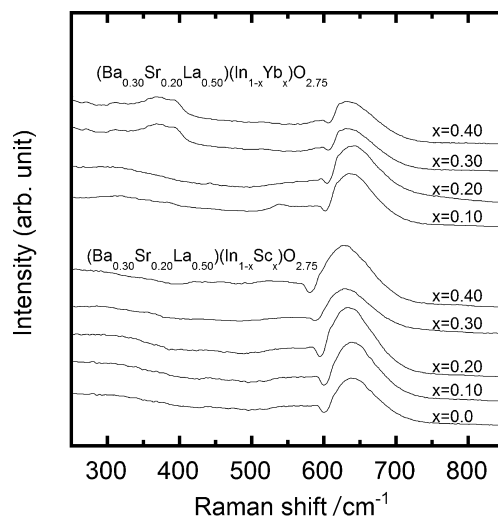


Fig. 7. Raman spectra of members of the  $(\text{Ba}_{0.3}\text{Sr}_{0.2}\text{La}_{0.5})(\text{In}_{1-x}\text{M}_x)\text{O}_{2.75}$  ( $\text{M} = \text{Sc}, \text{Yb}$ ) systems.

$- 0.4$ ). The  $\text{Cu K}\alpha$  XRD patterns showed that all the samples were single cubic phases. The oxide ion conductivities increased with the unit cell free volume up to  $2.43 \times 10^{-2} \text{ nm}^3$ , and then decreased with further volume increases. We conclude that the dependence of the conductivity on the unit cell free volume is related to the mobility of the oxide ions, because the oxygen vacancy content was maintained constant in the system. These results suggest that the oxide ion mobility of the system increases with the unit cell free volume; then, above a certain value, the mobility decreases due to the influence of other factors. Two Raman modes were detected in the  $(\text{Ba}_{0.3}\text{Sr}_{0.2}\text{La}_{0.5})(\text{In}_{1-x}\text{Yb}_x)\text{O}_{2.75}$  system, in which the unit cell free volume ranged above  $2.43 \times 10^{-2} \text{ nm}^3$ . The Raman mode of  $630 \text{ cm}^{-1}$  can be associated with oxygen vacancies in the perovskite oxide, and the other broad mode from  $350 \text{ cm}^{-1}$  to  $400 \text{ cm}^{-1}$  might relate to the local distortions of oxygen octahedra. Such local distortions may be responsible for the degradation of the oxide ion conductivity above unit cell free volumes of  $2.43 \times 10^{-2} \text{ nm}^3$ .

**Acknowledgement** This study was supported by the Scientific Frontier Research Project and Grant-in-Aid for Scientific Research from the Ministry of Education, Science, Sports and Culture, Japan.

#### References

- 1) T. Ishihara, J. Tabuchi, S. Ishikawa, J. Yan, M. Enoki and H. Matsumoto, *Solid State Ionics*, **177**, 1949–1953 (2006).
- 2) W. C. Maskell, *Solid State Ionics*, **134**, 43–50 (2000).
- 3) Y. Aizumi, H. Takamura, A. Kamegawa and M. Okada, *J. Ceram. Soc. Japan*, **112**, S724–S728 (2004).
- 4) T. Ishihara, T. Yamada, H. Arikawa, H. Nishiguchi and Y. Takita, *Solid State Ionics*, **135**, 631–636 (2000).
- 5) T. Ishihara, H. Matsuda and Y. Takita, *J. Am. Chem. Soc.*, **116**, 3801–3803 (1994).
- 6) T. Ishihara, H. Furutani, H. Arikawa, M. Honda, T. Akbay and Y. Takita, *J. Electrochem. Soc.*, **146**, 1643–1649 (1999).
- 7) J. B. Goodenough, J. E. Ruiz-Diaz and Y. S. Zhen, *Solid State Ionics*, **44**, 21–31 (1990).
- 8) T. Yao, Y. Uchimoto, M. Kinuhata, T. Inagaki and H. Yoshida, *Solid State Ionics*, **132**, 189–198 (2000).
- 9) Y. Uchimoto, T. Yao, H. Takagi, T. Inagaki and H. Yoshida, *Electrochemistry*, **68**, 531–533 (2000).
- 10) H. Kuramochi, T. Mori, H. Yamamura, H. Kobayashi and T.

- Mitamura, *J. Ceram. Soc. Japan*, **102**, 1159–1162 (1994).
- 11) K. Kakinuma, H. Yamamura, H. Haneda and T. Atake, *J. Thermal. Anal. Calorimetry*, **57**, 737–743 (1999).
- 12) K. Kakinuma, H. Yamamura, H. Haneda and T. Atake, *Solid State Ionics*, **140**, 301–306 (2001).
- 13) K. Kakinuma, H. Yamamura, H. Haneda and T. Atake, *Solid State Ionics*, **154–155**, 571–576 (2002).
- 14) K. Kakinuma, H. Yamamura and T. Atake, *J. Thermal. Anal. Calorimetry*, **69**, 897–904 (2002).
- 15) K. Kakinuma, N. Takahashi, H. Yamamura, K. Nomura and T. Atake, *Solid State Ionics*, **168**, 69–74 (2004).
- 16) T. Q. Ta, T. Tsuji and Y. Yamamura, *J. Alloy. Comp.*, **408–412**, 253–256 (2006).
- 17) H. Hayashi, H. Inaba, M. Matsuyama, N. G. Lan, M. Dokiya and H. Tagawa, *Solid State Ionics*, **122**, 1–15 (1999).
- 18) K. Nomura and S. Tanase, *Solid State Ionics*, **98**, 229–236 (1997).
- 19) R. D. Shannon, *Acta Cryst.*, **A32**, 751–753 (1976).
- 20) R. Chiba, F. Yoshimura and Y. Sakurai, *Solid State Ionics*, **124**, 281–288 (1999).
- 21) J. Mizusaki, T. Sasamoto, W. R. Cannon and H. K. Bowen, *J. Am. Ceram. Soc.*, **66**, 247–252 (1983).
- 22) A. Chainani, D. D. Sarma, I. Das and E. V. Sampathkumaran, *J. Phys. : Condens. Matter*, **8**, L631–L636 (1996).
- 23) H. Yamamura, H. Nishino, K. Kakinuma and K. Nomura, *Solid State Ionics*, **178**, 233–238 (2007).
- 24) J. A. Aguiar, D. A. L. Tellez, Y. P. Yadava and J. M. Ferreira, *Phys. Rev. B*, **58**, 2454–2457 (1998).
- 25) T. Scherban, R. Villeneuve, L. Abello and G. Lucaleau, *Solid State Ionics*, **61**, 93–98 (1993).
- 26) C. Chemarin, N. Rosman, T. Pagnier and G. Lucaleau, *J. Solid State Chem.*, **149**, 298–307 (2000).
- 27) I. Kosacki, J. Schoonman and M. Balkanski, *Solid State Ionics*, **57**, 345–351 (1992).
- 28) A. Mineshige, S. Okada, M. Kobune and T. Yazawa, *Solid State Ionics*, **177**, 2443–2445 (2006).
- 29) A. Mineshige, S. Okada, K. Sakai, M. Kobune, S. Fujii, H. Matsumoto, T. Shimura, H. Iwahara and Z. Ogumi, *Solid State Ionics*, **162–163**, 41–45 (2003).
- 30) N. Sata, H. Yugami, Y. Akiyama, H. Sone, N. Kitamura, T. Hattori and M. Ishigame *Solid State Ionics*, **125**, 383–387 (1999).